*Int. J. Heat Mass Transfer.* Vol. 33, No. 4, pp. 745–754, 1990
Printed in Great Britain

0017-9310/90 $3.00+0.00

# Solidification of a binary solution on a cold isothermal surface

S. L. BRAGA and R. VISKANTA

Heat Transfer Laboratory, School of Mechanical Engineering, Purdue University, West Lafayette, IN 47907, U.S.A.

(*Received* 27 *January* 1989 *and in final form* 18 *July* 1989)

**Abstract**—The freezing of water–salt solutions on a horizontal wall is investigated experimentally and theoretically. The growth of the two-phase solid–liquid region is observed for $NaCl–H_2O$ and $NH_4Cl–H_2O$ systems under different temperature and concentration conditions. A unidirectional mathematical model is developed to predict the temperature distribution in a semi-infinite medium based on the assumption that a local thermodynamic equilibrium exists between the solid and the liquid in the two-phase region. The transport of heat is by diffusion, and convection in the liquid is absent. The mass diffusion is neglected and the growth of the crystals is governed by the transport of heat. In all experiments the salt concentration in the solution is smaller than the eutectic composition, and the wall temperature is higher than the eutectic temperature. The predicted temperature profiles agree well with experimental data. The local solid fractions as well as the salt concentrations are shown as a function of the position.

## INTRODUCTION

THE PHASE change of multicomponent systems is important in many different fields such as metallurgy [1–4], geology [5], oceanography [6], crystal growth [7], nuclear reactor safety [8] and others. Almost all solid–liquid phase change processes involve more than one component. During the solidification of this type of system, the solid–liquid interface is not smooth as it is in the solidification of pure substances [9]. Normally, the transition from the liquid to the solid phase takes place over a range of temperatures and concentrations, while the chemical components are incorporated or rejected at the interface between the phases [10, 11]. This phenomenon changes the concentration of the system and determines the composition of the solid.

Figure 1 shows the phase diagram of a binary eutectic-forming melt [12, 13].This diagram represents the chemical compositions of the phases in thermodynamic equilibrium with each other by the liquidus and solidus, respectively. At a composition and temperature represented by a point above the liquidus line, the system is liquid. The solidus defines the composition of the material solidifying from the melt between the liquidus and the eutectic line. In general, the composition of the material differs from both the melt and the pure components of the system [1]. As shown in Fig. 1, solidification from a solution (melt) with subeutectic composition of $NH_4Cl$ in $H_2O$ yields a solid phase consisting of a pure component (ice). The solid and the liquid phases can coexist at the same temperature and different compositions, which are determined by the solidus and the liquidus lines. This region is usually called the mushy zone or simply mush. For most aqueous solutions, the solidus line is vertical and the solid phase in the mushy region is composed of a single component (ice), while the salt is rejected to the melt increasing its concentration.

This work has been motivated by the need to understand the solidification process in the mushy zone under stable conditions with cooling the solidifying melt from below. Fang *et al.* [8], working with sodium chloride–water solution, investigated the growth of a mushy region over an ice slab. In their study, the temperature of the ice slab was not constant, particularly at late times (1 h or greater), and, therefore, the boundary condition is not well defined. Huppert and Worster [14] also studied the solidification of $Na_2CO_3$–water solutions and compared their predictions with the experimental data. In their model, however, the solid fraction in the mush was assumed to be constant and the latent heat of fusion was released at the interface. In this paper we develop a mathematical model to predict the solidification of an aqueous solution of subeutectic composition. In order to validate the theory, an experimental investigation was conducted using two different salt solutions: $NaCl–H_2O$ and $NH_4Cl–H_2O$. In the case of the sodium chloride–water solution, the choice was motivated by the fact that it is a very common solution and its thermophysical properties are well established [13]. The ammonium chloride–water solution was chosen because in the past it was utilized as a model system to study dendritic solidification [15]. Three different concentrations (5, 10 and 15% by weight) were tested for each salt, involving a wide composition range.

## NOMENCLATURE

| | |
|---|---|
| $C$ | solution concentration |
| $c$ | specific heat |
| $f$ | solid fraction in the two-phase region |
| $\Delta h_f$ | latent heat of fusion |
| $k$ | thermal conductivity |
| $Ste$ | Stefan number, $\Delta h_f/c_s(T_m - T_w)$ |
| $T$ | temperature |
| $t$ | time |
| $x$ | vertical coordinate measured from the surface of the heat exchanger. |

Greek symbols

| | |
|---|---|
| $\alpha$ | thermal diffusivity |
| $\delta$ | thickness of the two-phase region |
| $\eta$ | similarity coordinate, equation (8) |
| $\theta$ | dimensionless temperature, equation (7) |
| $\theta_0$ | dimensionless initial temperature, $(T_0 - T_\delta)/(T_\delta - T_w)$ |
| $\theta_\delta$ | dimensionless liquidus temperature, $T_\delta/(T_\delta - T_w)$ |
| $\rho$ | density |
| $\sigma$ | solidification constant, equation (11). |

Subscripts

| | |
|---|---|
| l | liquid region |
| m | two-phase region |
| s | solid region |
| w | conditions at the wall ($x = 0$) |
| 0 | initial conditions |
| $\delta$ | liquidus condition ($C = C_0$). |

Superscripts

| | |
|---|---|
| $'$ | derivative with respect to $\eta$ |
| * | dimensionless quantities normalized by the liquid properties. |

## EXPERIMENTAL APPARATUS AND PROCEDURE

Solidification experiments were performed in a rectangular test cell with inner dimensions, 300 mm in height, 150 mm in width, and 75 mm in depth. Figure 2 shows schematically the experimental apparatus.

The horizontal bottom consisted of a multipass copper heat exchanger that was plated with nickel and chrome to avoid corrosion by the salt. Three copper–constantan thermocouples (type T) were placed close to the heat-transfer surface continuously monitoring its temperature. The vertical test cell walls were made of acrylic sheets in order to allow the visualization and the growth of the mushy zone. The test cell was well insulated with 50 mm thick Styrofoam insulation on all sides to reduce heat gain from the ambient.

Measurements of the temperature distribution inside the test cell were made also with (type T) thermocouples. They were placed in stainless steel tubes having outside diameter of 0.90 mm. These probes were inserted through one of the walls where 21 holes allowed the installation of the thermocouples in several positions. Typically, six probes were used in each experiment. The outputs of all the thermocouples were recorded by a data logger system at preselected time intervals between two consecutive measurements.

A mixture of ethyl alcohol and water from a constant temperature bath was used in the heat exchanger to obtain the desired wall temperature. During all the experiments it was possible to maintain this temperature uniform to within ±0.1°C of the desired value. Due to the transient nature of the experiments, the temperature setting of the bath was frequently readjusted.

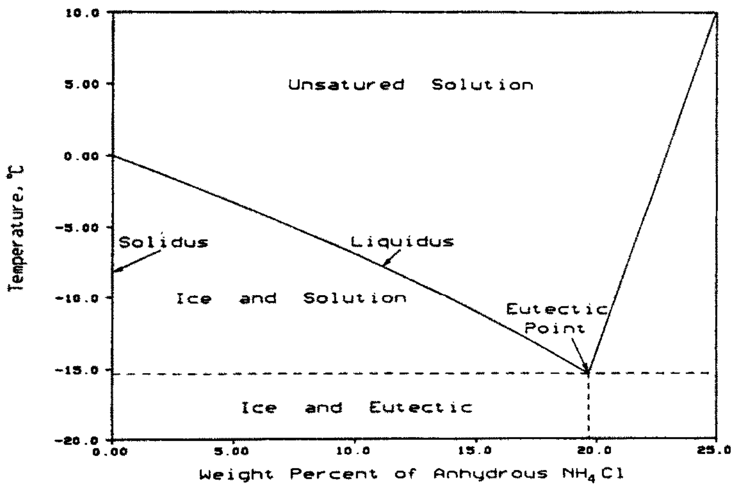

FIG. 1. Phase diagram of an aqueous $NH_4Cl$ solution.

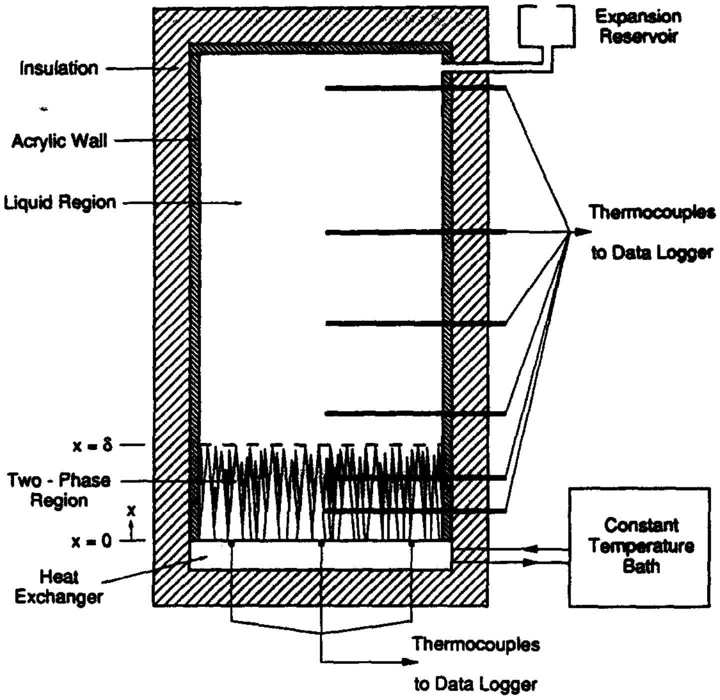

FIG. 2. Schematic diagram of the test cell.

Experiments were performed with distilled water–research grade salt solution and its concentrations, in all cases, were smaller than the eutectic composition. These mixtures were carefully introduced into the test cell without introducing air bubbles into the system. An expansion reservoir was installed in the upper part of the apparatus (see Fig. 2) to allow for expansion and contraction of the phase change material. Once filled, enough time was allowed to reach the thermal equilibrium in the test cell. Then, the coolant from the constant temperature bath was circulated through the heat exchanger to start the experiment.

## ANALYTICAL MODEL

The mathematical model for the solidification process of a binary system is based on the basic conservation principles. A macroscopic model is constructed to determine theoretically the rate of solidification and predict the temperature distribution in the system if the solid/melt interface is perfectly flat and horizontal.

During the solidification process, the solution near the ice surface rejects the solute. In this way, a more dense and cold solution appears in the mushy zone. Because of this, the liquid phase is hydrodynamically stable and there is no convective motion in the fluid. The liquid region is considered to be semi-infinite extent in the vertical direction. In order to simplify the analysis, it is assumed that the growth of the two-phase region is controlled by heat conduction. This assumption is based on the fact that the thermal diffusivity of the salt solutions is two orders of magnitude greater than the mass diffusivity [8, 12, 14]. In addition, both the mushy and the liquid regions are treated as a continuum and the problem is one-dimensional. In other words, the thermophysical properties in the two-phase region are assumed to be constant in the horizontal plane as an average between the two phases. It is supposed also that the local thermodynamic equilibrium exists in the same horizontal plane (solid and liquid are at the same temperature). Hence, the temperature and concentration of the solution follow the liquidus curve of the respective phase diagram. Finally, the change in the density during the solidification is neglected, and all thermophysical properties are constant within the liquid and solid, but different from each other in the two phases.

With the above assumptions, the model equations describing the temperature distributions are

$$\rho_m \frac{\partial}{\partial t}(c_m T) = \frac{\partial}{\partial x}\left(k_m \frac{\partial T}{\partial x}\right) + \rho_m \Delta h_f \frac{\partial f}{\partial t}, \quad 0 \leqslant x \leqslant \delta \qquad (1)$$

$$\rho_l c_l \frac{\partial T}{\partial t} = k_l \frac{\partial^2 T}{\partial x^2}, \quad x \geqslant \delta. \qquad (2)$$

The initial ($t = 0$) conditions are

$$T = T_0 \qquad (3a)$$

$$\delta = 0 \qquad (3b)$$

and the boundary conditions are

$$T = T_0, \quad x \to \infty \tag{4a}$$

$$T = T_w, \quad x = 0 \tag{4b}$$

$$T = T_\delta, \quad x = \delta \tag{4c}$$

$$k_l \left.\frac{\partial T}{\partial x}\right|_{\delta_+} = k_m \left.\frac{\partial T}{\partial x}\right|_{\delta_-}. \tag{4d}$$

The thermophysical properties in the mushy zone are weighted according to the local solid fraction [16] as follows:

$$\rho_m = \rho_l = \rho_s \tag{5a}$$

$$c_m = f(c_s - c_l) + c_l \tag{5b}$$

$$k_m = f(k_s - k_l) + k_l. \tag{5c}$$

The local solid fraction can be determined from the phase diagram by

$$f = \frac{C(T) - C_0}{C(T)} \tag{6}$$

where $C(T)$ is obtained directly from the liquidus line.

In order to generalize the problem, the following dimensionless variables are introduced:

$$\theta = \frac{T - T_\delta}{T_\delta - T_w} \tag{7}$$

and

$$\eta = \frac{x}{\sqrt{(4\alpha_l t)}}. \tag{8}$$

Then, the dimensionless system of equations becomes

$$2\left\{[f(c_s^* - 1) + 1] + [(c_s^* - 1)(\theta + \theta_\delta) - Ste]\frac{\partial f}{\partial \theta}\right\}\eta\theta' + (k_s^* - 1)\frac{\partial f}{\partial \theta}\theta'^2 + [(k_s^* - 1)f + 1]\theta'' = 0,$$

$$0 \leqslant \eta \leqslant \sigma \tag{9}$$

and

$$\theta'' + 2\eta\theta' = 0, \quad \eta \geqslant \sigma \tag{10}$$

where

$$\sigma = \frac{\delta}{\sqrt{(4\alpha_l t)}}. \tag{11}$$

The transformed initial and boundary conditions become as follows:

$$\theta = \theta_0, \quad \eta \to \infty \tag{12a}$$

$$\theta = -1, \quad \eta = 0 \tag{12b}$$

$$\theta = 0, \quad \eta = \sigma \tag{12c}$$

$$\theta'(\sigma_+) = \theta'(\sigma_-). \tag{12d}$$

In equations (9), (10) and (12d) the superscript prime denotes the total derivative with respect to $\eta$.

The exact analytical solution of equation (10) is

$$\theta = \theta_0\left(1 - \frac{\operatorname{erfc}\eta}{\operatorname{erfc}\sigma}\right). \tag{13}$$

This solution is valid for $\eta \geqslant \sigma$ and satisfies the boundary conditions (12a) and (12c). The derivative of $\theta$ with respect to $\eta$ at the interface is

$$\theta' = \frac{2\theta_0\,e^{-\sigma^2}}{\pi^{1/2}\operatorname{erfc}\sigma} \tag{14}$$

but the value of $\sigma$ is not known.

To find the dimensionless temperature in the mushy region from equation (9), it is necessary to know the relation between the solid fraction $f$ and the dimensionless temperature $\theta$ as well as its derivative. Using equations (6) and (7) and the phase diagram [12, 13], the $f$ vs $\theta$ functional relationship can be determined. A third degree polynomial obtained by a least squares fit is used. A finite-difference method is employed, with an initial estimated value for $\sigma$ to find the dimensionless temperature distribution in the mushy zone. The boundary conditions, given by equations (12b) and (12c), are also satisfied. Then, an iterative procedure is employed until the final value of $\sigma$ is determined. At this location, the derivative of the function found from equation (9) is equal to the value given by equation (14), thus satisfying the boundary condition prescribed by equation (12d).

## RESULTS AND DISCUSSION

Six different experiments were performed using water solutions of 5, 10 and 15% by weight of NaCl and $NH_4Cl$. Table 1 shows the initial concentration and the initial and wall temperatures for each experiment. The duration of each test ($t_d$) and the maximum time ($t_{max}$) during which the liquid region may be regarded as a semi-infinite medium are also listed in the table. In all experiments, the initial temperature was determined as an average of the measured temperatures within a range of ±0.1°C. The same procedure was used for the wall temperature after first waiting 15 min to obtain stable conditions. Typically, the desired temperature was reached in less than 5 min.

Dendritic crystal growth was observed in all cases. The mushy region for 5% concentration of both salt solutions is shown in Fig. 3. It is clearly evident from

Table 1. Test conditions for the experiments

| Salt solution | $C_0$ (%) | $T_0$ (°C) | $T_w$ (°C) | $t_d$ (min) | $t_{max}$ (min) |
|---|---|---|---|---|---|
| | 5 | 22.7 | −19.2 | 420 | 590 |
| NaCl | 10 | 21.9 | −17.8 | 540 | 620 |
| | 15 | 21.2 | −19.4 | 540 | 650 |
| | 5 | 15.3 | −13.3 | 500 | 630 |
| $NH_4Cl$ | 10 | 20.2 | −14.6 | 540 | 640 |
| | 15 | 19.5 | −14.7 | 540 | 660 |

the photographs for the two solutions that there is a large difference between the structures (see Figs. 3(a) and (b)) for the two binary systems. However, during the experiments it was possible to see that the shapes of isolated crystals are very similar for both NaCl and $NH_4Cl$ solutions. This can be partly explained by the fact that in both cases the crystals growing are ice. Figure 3(c) shows a closer view of the mush in the experiment with ammonium chloride solution, while Fig. 3(d) shows a close-up of one crystal under the same conditions. It is possible to see that there is a difference in the refractive index of the solution caused by the release of the salt during the process of solidification.

During the tests the insulation used to reduce the heat gains from the ambient environment did not allow for visualization of the solidification process. However, once during each test, a window in the Styrofoam was opened in order to examine the interface position. Two scales located on the front and the

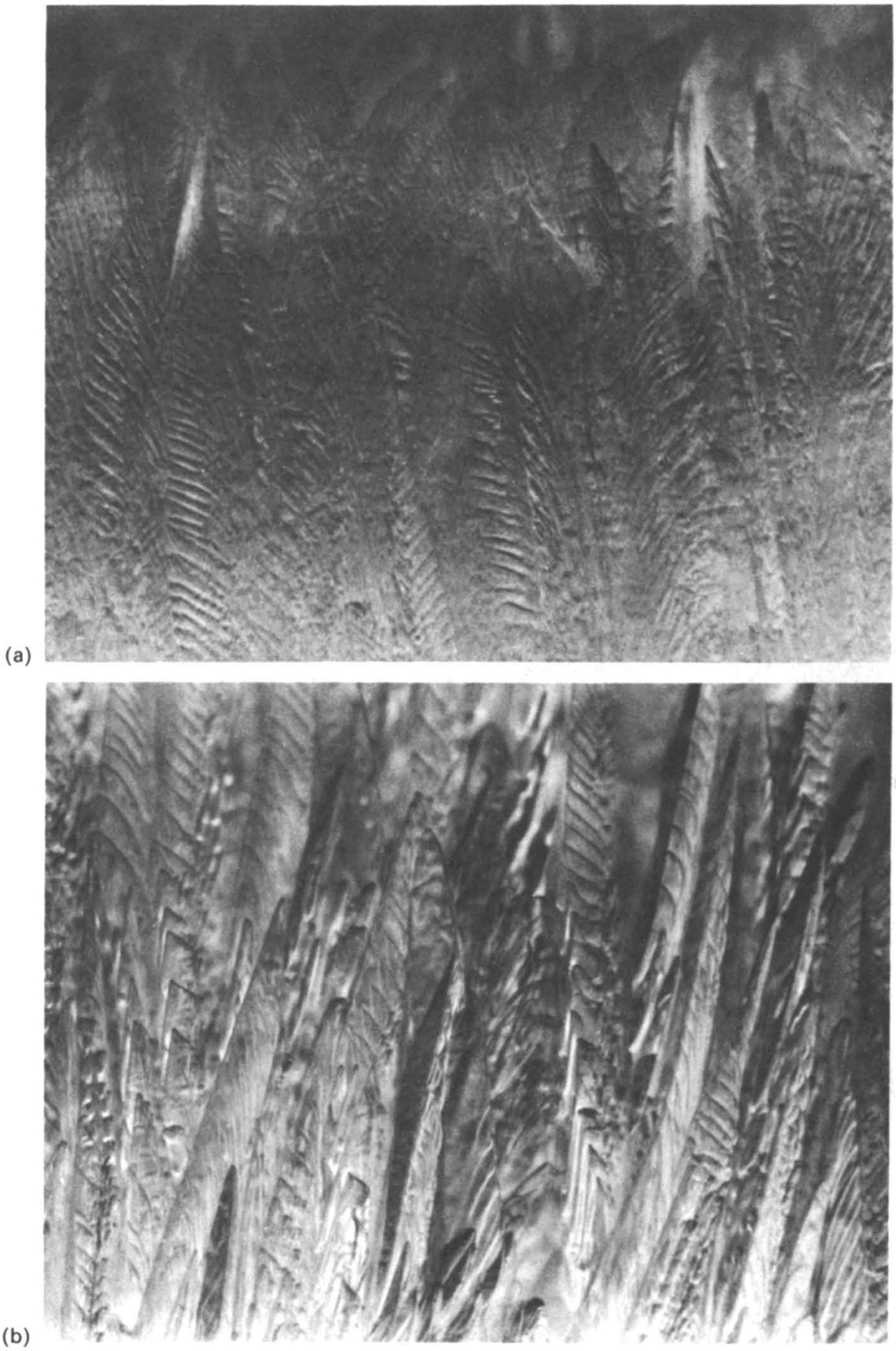

FIG. 3. Different views of dendritic crystals in the two-phase region: (a) $NaCl–H_2O$; (b) $NH_4Cl–H_2O$; (c) $NH_4Cl–H_2O$ closer view; (d) $NH_4Cl–H_2O$ close-up view.

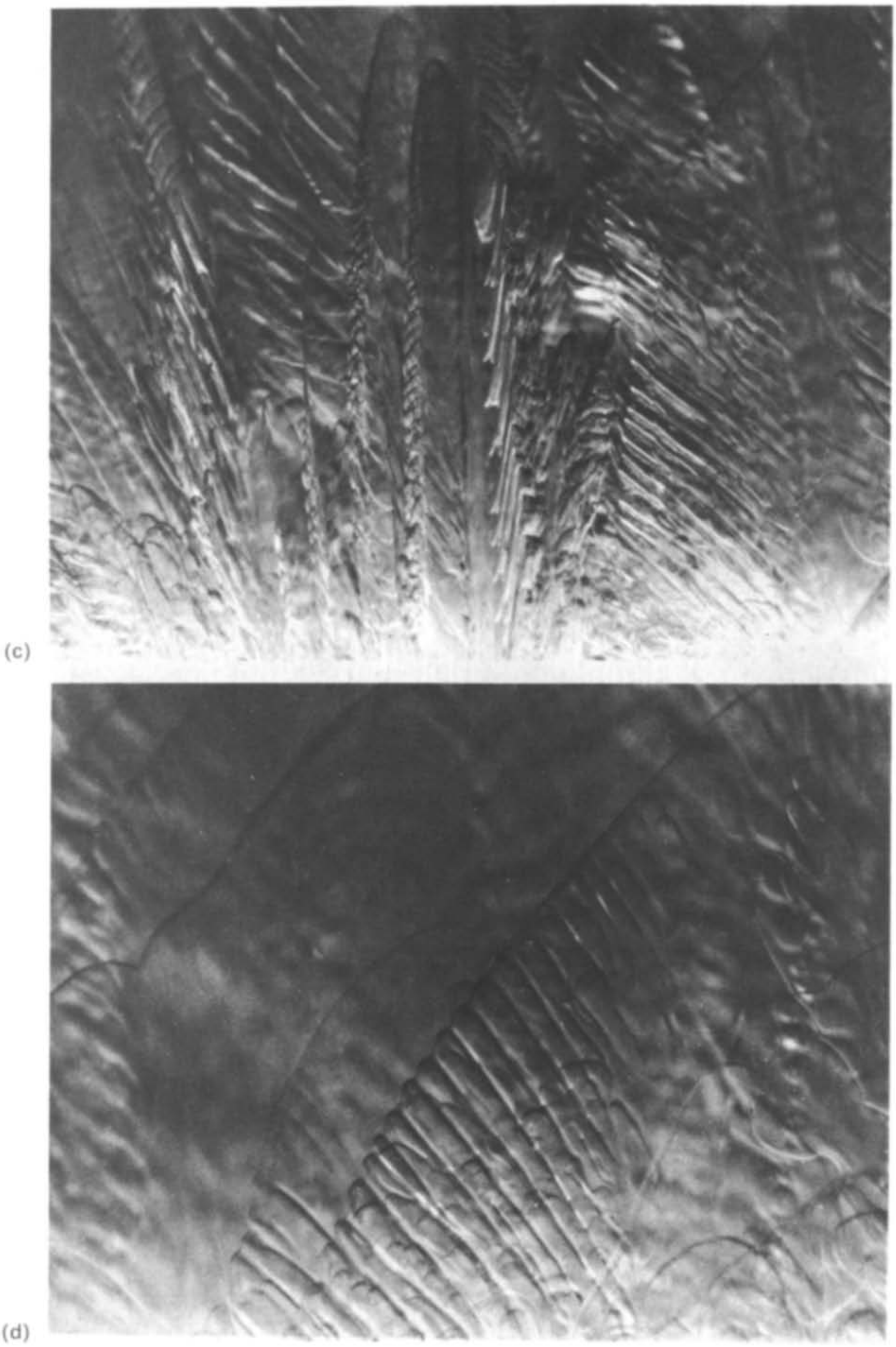

FIG. 3—*continued.*

back walls of the test cell were used in this measurement. The mush–liquid interfaces were quite flat in the experiments with the lower salt solution concentrations. For the largest initial concentrations, the interfaces were not as uniform but were within $\pm 0.5$ mm. However, it was very easy to measure the average thickness of the two phase regions for all cases investigated. Table 2 gives a comparison of the predicted and measured positions of $\delta$ at the time the observations were made. The agreement with the 5% composition of the salt solution is good, while the discrepancy increases for larger concentrations of salt in the solution.

A comparison of the measured and predicted dimensionless temperature distributions in the systems are shown in Figs. 4 and 5. The continuous lines represent the theoretical predictions, while the points are the experimental data. In all cases, the plotted data points were obtained from $t = 15$ min till $t = t_d$ (shown in Table 1). In order to better resolve the comparisons in the mushy zone, the two-phase region was enlarged and is shown in Figs. 4(b) and 5(b). The

Table 2. Comparison of predicted and measured interface positions

| Salt solution | $C_0$ (%) | $t$ (min) | $\delta$ (mm) Theoretical | Experimental |
|---|---|---|---|---|
| | 5 | 420 | 57.0 | 56.0 |
| NaCl | 10 | 540 | 47.8 | 45.0 |
| | 15 | 380 | 28.2 | 22.0 |
| | 5 | 500 | 51.0 | 48.0 |
| $NH_4Cl$ | 10 | 540 | 36.6 | 32.0 |
| | 15 | 540 | 16.3 | 13.0 |

good agreement between the experimental data and the predictions obtained from the theoretical model proves that the assumptions made in the analysis are valid.

With the assumption of thermodynamic equilibrium and the temperature profile in the mush it is possible to establish a relation between the dimensionless position and the solid fraction. The same procedure can be used to find the local concentration as a function of the transformed position. These relations are shown in Figs. 6 and 7 for the three experiments with the $NaCl–H_2O$ solution. It is interesting to note that the concentration of the solution close to the isothermal wall is a function of its temperature only, while the solid fraction depends also on the initial concentration. This appears clearly from the results shown in Figs. 6 and 7. If the wall temperatures are close in these experiments (see Table 1) the concentrations near the heat exchanger are also close. On the other hand, the solid fractions are totally different, because the initial concentrations are so distinct from one another.

From Figs. 4 to 7 it is clear that with an increase in the salt concentration in the solution, the rate of growth of the mushy zone decreases. This is explained by the freezing point depression which increases with an increase in the salt concentration of a binary melt, lowering the temperature of the mush–liquid interface. As expected, a decrease in the wall temperature increased the freezing rate. It was also verified that the initial temperature affects the growth of the two-phase region in the same way as the concentration.

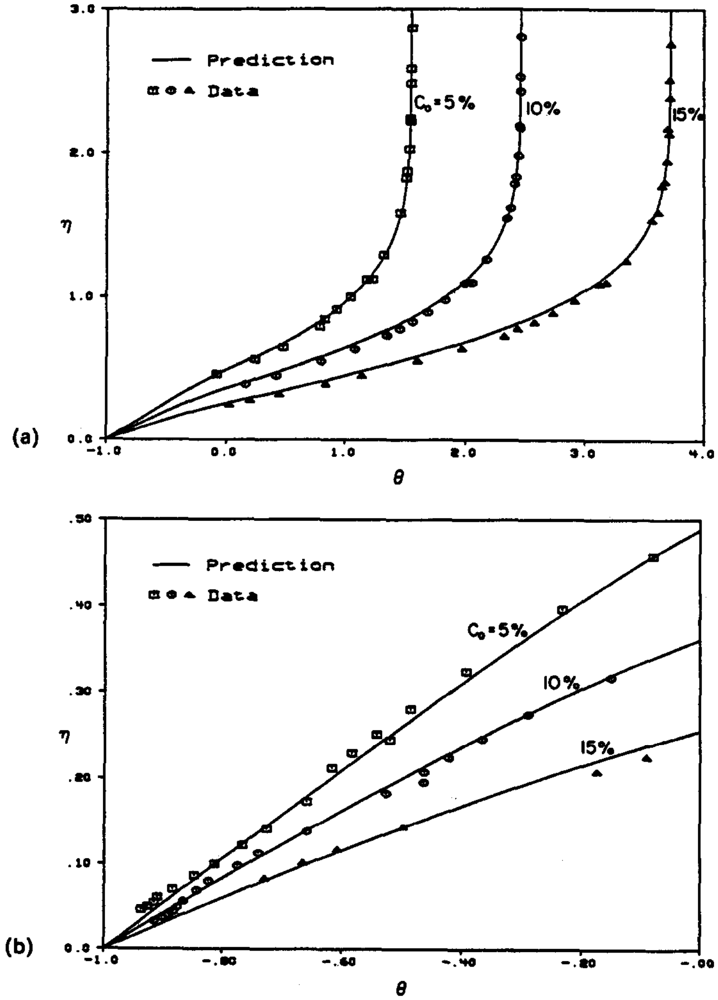

FIG. 4. Comparison of predicted and measured temperature distributions during solidification of $NaCl–H_2O$ solutions: (a) liquid region; (b) two-phase region.

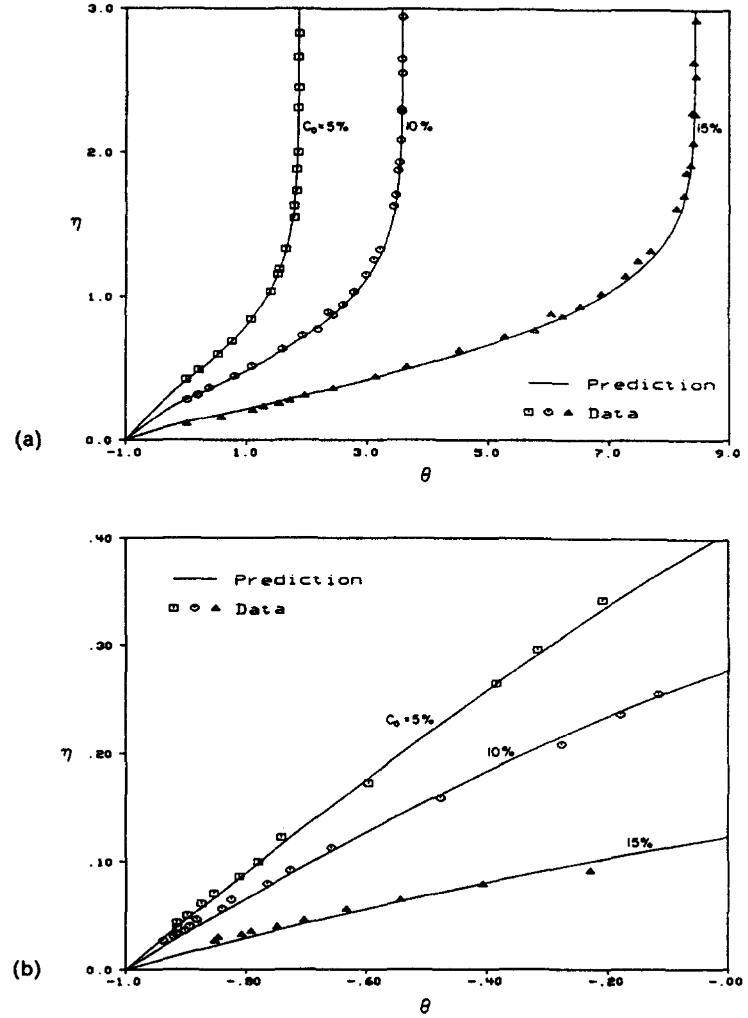

FIG. 5. Comparison of predicted and measured temperature distributions during solidification of $NH_4Cl$–$H_2O$ solutions: (a) liquid region; (b) two-phase region.

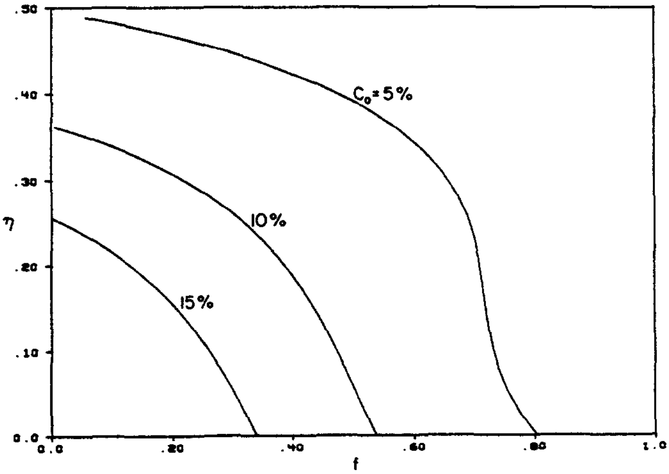

FIG. 6. Predicted distribution of the solid fraction in the two-phase region for NaCl–$H_2O$ solutions.

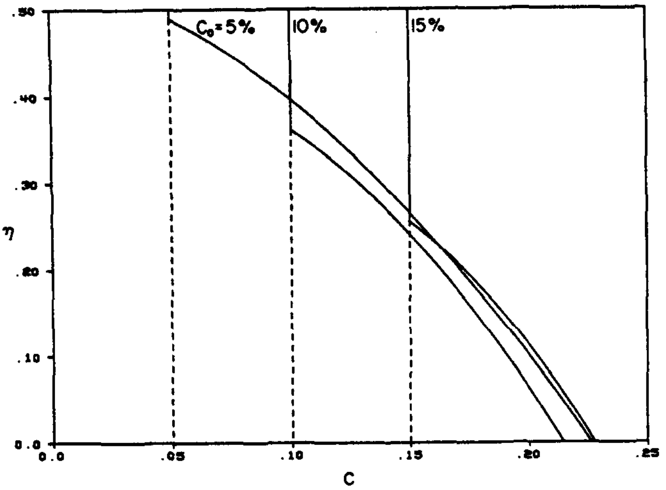

FIG. 7. Predicted concentration distribution in the two-phase region during solidification of NaCl–$H_2O$ solutions.

Comparisons with other works show that, as expected, the same behavior occurs in experiments with different salts and experimental techniques. Huppert and Worster [14] used $NaCO_3$, and their measurements have shown that the concentration of the salt solution in the mush increases while in the liquid region it remains constant. Fang *et al.* [8] using an ice slab as a cold surface, found a similar temperature and the same type of solid fraction distribution in the mushy zone as was observed in the present work. Direct comparison with their results cannot be made, because the surface temperature of the sink was not held constant in their experiments.

## CONCLUDING REMARKS

A model describing the temperature distribution during solidification from below of subeutectic aqueous solutions has been developed. Comparison between predictions and experimental results proves that the assumptions are reasonable, and the agreement is good. The concentration of the solution was found to be as important as the initial and the wall temperatures as far as the growth of the mushy zone was concerned. The knowledge of the temperature distribution and the thermodynamic equilibrium assumption yielded the local solid fraction as well as the local solution concentration in the mushy region.

*Acknowledgements*—This work was carried out when one of the authors (S. L. B.) held a visiting appointment at Purdue University. He would like to express his appreciation to the Pontificia Universidade Catolica do Rio de Janeiro and the Conselho Nacional de Desenvolimento Cientifico e Tecnologico for supporting his sabbatical leave during 1988–89.

## REFERENCES

1. M. C. Flemings, *Solidification Processing*. McGraw-Hill, New York (1974).
2. S. M. Copley, A. F. Giamei, S. M. Johnson and M. F. Hornbecker, The origin of freckles in unidirectionally solidified casting, *Metall. Trans.* **1**, 2193–2204 (1970).
3. I. Minkoff, *Solidification and Cast Structure*. Wiley, New York (1986).
4. T. J. Smith, *Modeling the Flow and Solidification of Metals*. Martinus Nijhoff, Dordrecht, The Netherlands (1987).
5. H. E. Huppert and R. S. J. Sparks, Double-diffusive convection due to crystalization of magma. In *Annual Review of Earth and Planetary Science* (Edited by G. W. Weitherill, A. L. Albee and F. G. Stehli), Vol. 12, pp. 11–37. Annual Reviews, Inc., Palo Alto, California (1984).
6. P. V. Hobbs, *Ice Physics*. Clarendon Press, Oxford (1974).
7. W. Bardsley, D. T. J. Hurle and T. B. Mullin, *Crystal Growth: a Tutorial Approach*. North-Holland, Amsterdam (1979).
8. L. J. Fang, F. B. Cheung, J. H. Linehan and D. R. Pedersen, Selective freezing of a dilute salt solution on a cold ice surface, *J. Heat Transfer* **106**, 385–393 (1984).
9. R. Viskanta, Phase-change heat transfer. In *Solar Heat Storage: Latent Heat Materials* (Edited by J. A. Lane), Vol. 1, Chap. V, pp. 153–222. CRC Press, Boca Raton, Florida (1983).
10. S. Chellaiah and R. Viskanta, Freezing of salt solution on a vertical wall, *Expl Heat Transfer* **1**, 181–195 (1988).
11. R. Viskanta and C. Beckermann, Modeling of transport phenomena during solidification. In *Interdisciplinary Issues in Materials Processing* (Edited by S. K. Samanta, R. Komandouri, R. McKeeking, M. M. Chen and A. Tseng), Vol. 2, pp. 501–526. ASME, New York (1987).
12. *International Critical Tables of Numerical Data, Physics, Chemistry and Technology*, Vol. 3, p. 60 and Vol. 4, p. 218. National Research Council U.S., McGraw-Hill, New York (1933).
13. *Saline Water Conversion Engineering Data Book*. M. W. Kellogg Company, New York (1965).
14. H. E. Huppert and M. G. Worster, Dynamic solidification of a binary melt, *Nature* **314**, 703–707 (1985).
15. J. Szekely and A. S. Jassal, An experimental and analytical study of solidification of a binary dendritic system, *Metall. Trans.* **9B**, 389–398 (1978).
16. G. K. Batchelor, Transport properties of two-phase materials with random structure, *Ann. Rev. Fluid Mech.* **6**, 227–255 (1974).

# SOLIDIFICATION D'UNE SOLUTION BINAIRE SUR UNE SURFACE ISOTHERME FROIDE

**Résumé**—Le gel de solutions salines d'eau sur une paroi horizontale est étudié expérimentalement et théoriquement. La croissance de la région diphasique solide–liquide est observée pour $NaCl–H_2O$ et $NH_4Cl–H_2O$ à différentes températures et différentes concentrations. Un modèle mathématique unidirectionnel est développé pour prédire la distribution de température dans un milieu semi-infini, en admettant qu'il existe un équilibre thermodynamique local entre le solide et le liquide dans la région diphasique. Le transfert de chaleur par diffusion et convection dans le liquide est absent. La diffusion de masse est négligée et la croissance des cristaux est gouvernée par le transfert thermique. Dans toutes les expériences la concentration en sel dans la solution est plus faible que la composition eutectique et la température de la paroi est supérieure à la température eutectique. Les profils de température calculés s'accordent bien avec les données expérimentales. Les fractions locales de solide ainsi que les concentrations en sel sont donnees en fonction de la position.

# VERFESTIGUNG EINER BINÄREN LÖSUNG AN EINER KALTEN ISOTHERMEN OBERFLÄCHE

**Zusammenfassung**—Das Gefrieren von Wasser/Salz-Lösungen an einer horizontalen Wand ist experimentell und theoretisch untersucht worden. Das Anwachsen des zweiphasigen fest-flüssigen Gebietes wurde für $NaCl–H_2O$- und $NH_4Cl–H_2O$-Systeme bei verschiedenen Temperatur- und Konzentrationsbedingungen beobachtet. Ein einseitiges mathematisches Modell ist entwickelt worden, um die Temperaturverteilung in einem halbunendlichen Medium zu berechnen, und zwar aufgrund der Annahme, daß zwischen fester und flüssiger Phase lokales thermodynamisches Gleichgewicht besteht. Der Wärmetransport erfolgt durch Wärmeleitung ohne Konvektion in der Flüssigkeit. Die Diffusion wird vernachlässigt, und das Kristallwachstum wird vom Wärmetransport gesteuert. Bei allen Experimenten ist die Salzkonzentration in der Lösung kleiner als die der eutektischen Mischung, und die Wandtemperatur ist höher als die eutektische. Die berechneten Temperaturprofile stimmen mit den gemessenen gut überein. Der lokale Festkörperanteil und die Salzkonzentrationen werden abhängig von der Position dargestellt.

# ЗАТВЕРДЕВАНИЕ БИНАРНОГО РАСТВОРА НА ХОЛОДНОЙ ИЗОТЕРМИЧЕСКОЙ ПОВЕРХНОСТИ

**Аннотация**—Экспериментально и теоретически исследуется замерзание водо-солевых растворов на горизонтальной стенке. В системах $NaCl–H_2O$ и $NH_4Cl–H_2O$ при различных температурах и концентрациях наблюдается образование двухфазной области твердое тело–жидкость. На основе допущения о том, что в двухфазной области твердое тело и жидкость находятся в термодинамическом равновесии, разработана математическая модель для расчета распределения температуры в полубесконечной среде. Тепло переносится за счет диффузии, конвекция в жидкости отсутствует. Диффузия массы не учитывается, и рост кристаллов определяется переносом тепла. Во всех экспериментах концентрация соли в растворе была ниже, чем в эвтектическом составе, а температура стенки выше эвтектической температуры. Расчетные профили температуры хорошо согласуются с экспериментальными данными. Локальные доли твердого вещества, а также концентрация соли представлены как функции координат.